ISSN 1420-9101

JOURNAL OF Evolutionary Biology

VOLUME 33 ISSUE 3 MARCH 2020

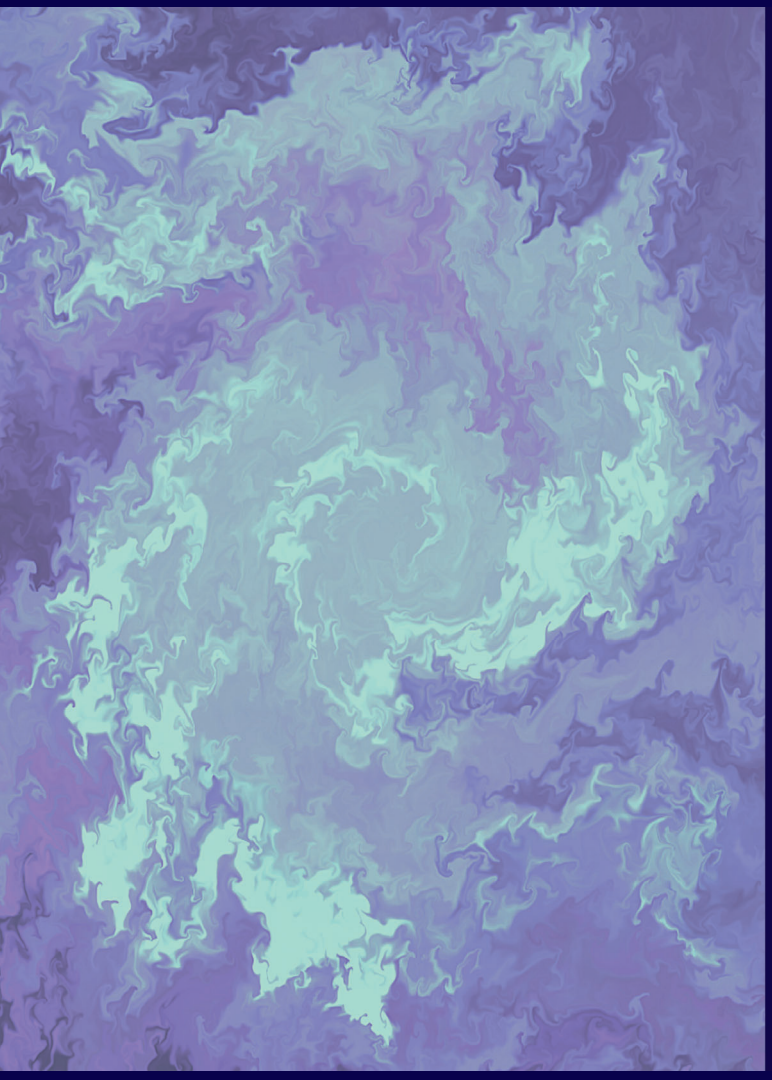

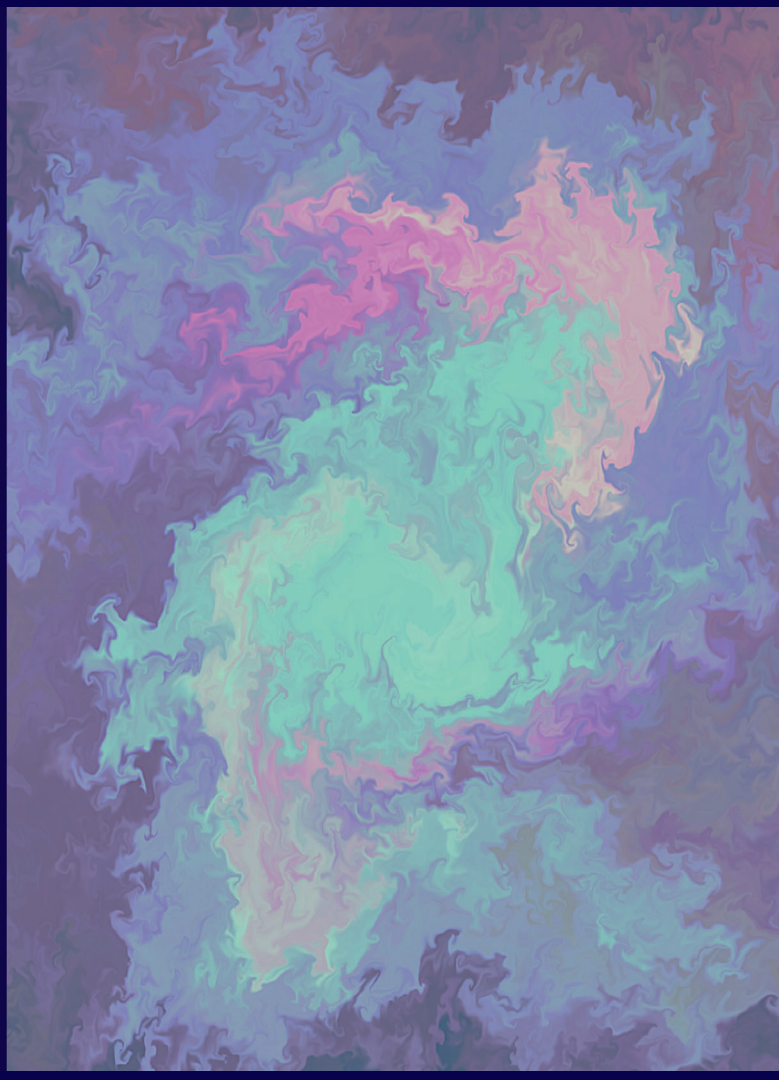

WILEY Blackwell

eseb European Society for Evolutionary Biology

Journal of
EVOLUTIONARY BIOLOGY

For the European Society for Evolutionary Biology

Aims and Scope *Journal of Evolutionary Biology* is a monthly, peer-reviewed, international journal. It covers both micro- and macro-evolution of all types of organisms. The aim of the journal is to integrate perspectives across molecular and microbial evolution, behaviour, genetics, ecology, life histories, development, palaeontology, systematics and morphology. To fulfil its integrative role, the journal gives preference to papers that bring together two or more fields. The journal seeks a balance, even a tension, between theory and data. The Editorial Board reflects the multidisciplinary role of the Journal and its international focus.

Online Open *Journal of Evolutionary Biology* accepts articles for Open Access publication. Please visit http://olabout.wiley.com/WileyCDA/Section/id-828081.html. for further information about OnlineOpen.

Information for Subscribers The *Journal of Evolutionary Biology* is published in 12 issues per year. Institutional subscription prices for 2020 are: Online Only: £2,284 (UK), US$4,252 (US), US$4,252 (Rest of World), €2,900 (Europe). Prices are exclusive of tax. Asia-Pacific GST, Canadian GST/HST and European VAT will be applied at the appropriate rates. For more information on current tax rates, please go to https://onlinelibrary.wiley.com/library-info/products/price-lists/payment. The price includes online access to the current and all online backfiles to January 1st 2013, where available. For other pricing options, including access information and terms and conditions, please visit https://onlinelibrary.wiley.com/library-info/products/price-lists.

Terms of use can be found here: https://onlinelibrary.wiley.com/terms-and-conditions

Note to NIH Grantees Pursuant to NIH mandate, Wiley Blackwell will post the accepted version of contributions authored by NIH grant-holders to PubMed Central upon acceptance. This accepted version will be made publicly available 12 months after publication. For further information, see www.wiley.com/go/nihmandate.

Delivery Terms and Legal Title Where the subscription price includes print issues and delivery is to the recipient's address, delivery terms are Delivered at Place (DAP); the recipient is responsible for paying any import duty or taxes. Title to all issues transfers FOB our shipping point, freight prepaid. We will endeavour to fulfil claims for missing or damaged copies within six months of publication, within our reasonable discretion and subject to availability.

Back Issues Single issues from current and recent volumes are available at the current single issue price from cs-journals@wiley.com. Earlier issues may be obtained from Periodicals Service Company, 351 Fairview Avenue – Ste 300, Hudson, NY 12534, USA. Tel: +1 518 822-9300, Fax: +1 518 822-9305, Email: psc@periodicals.com

Periodical ID Statement *JOURNAL OF EVOLUTIONARY BIOLOGY* (ISSN 1420-9101) is published monthly.

Publisher *Journal of Evolutionary Biology* is published by John Wiley & Sons Ltd., 9600 Garsington Road, Oxford OX4 2DQ, UK, Tel: +44 1865 776868, Fax: +44 1865 714591, Email: customer@wiley.com.

Journal Customer Services For ordering information, claims and any enquiry concerning your journal subscription please go to https://hub.wiley.com/community/support/onlinelibrary or contact your nearest office: **Americas:** E-mail: cs-journals@wiley.com; Tel: +1 781 388 8598 or +1 800 835 6770 (toll free in the USA & Canada). **Europe, Middle East and Africa:** E-mail: cs-journals@wiley.com; Tel: +44 (0) 1865 778315. **Asia Pacific:** E-mail: cs-journals@wiley.com; Tel: +65 6511 8000. **Japan:** For Japanese speaking support, E-mail: cs-japan@wiley.com; Tel: +65 6511 8010 or Tel (toll-free): 005 316 50 480. **Visit our Online Customer Help** at https://hub.wiley.com/community/support/onlinelibrary

View this journal online at wileyonlinelibrary.com/journal/jeb.

Wiley is a founding member of the UN-backed HINARI, AGORA, and OARE initiatives. They are now collectively known as Research4Life, making online scientific content available free or at nominal cost to researchers in developing countries. Please visit Wiley's Content Access – Corporate Citizenship site: http://www.wiley.com/WileyCDA/Section/id-390082.html

Abstracting and Indexing Services The Journal is indexed by Animal Behaviour Abstracts, Biological Abstracts, BIOSIS, CAB International, CABS (Current Awareness in Biological Sciences), Cambridge Scientific Abstracts, Chemical Abstracts, Current Contents, Entomology Abstracts, Geo Abstract and Scopus. The full list is published on the journal home pages.

Wiley's Corporate Citizenship initiative seeks to address the environmental, social, economic, and ethical challenges faced in our business and which are important to our diverse stakeholder groups. Since launching the initiative, we have focused on sharing our content with those in need, enhancing community philanthropy, reducing our carbon impact, creating global guidelines and best practices for paper use, establishing a vendor code of ethics, and engaging our colleagues and other stakeholders in our efforts. Follow our progress at www.wiley.com/go/citizenship

For submission instructions, subscription and all other information visit: http://www.journalofevolutionarybiology.org

An EndNote style file is available from http://authorservices.wiley.com/jendnotes/. We have endeavoured to make this style file as comprehensive as possible, but complex or unusual reference types and variations in reference data quality in EndNote may result in missing information or formatting problems. If you have any comments or suggestions for improvement, please contact the journal Production Editor at: jeb@wiley.com

Specifications

Tables Tables should be cited consecutively in the text and labelled (Table 1, Table 2, etc.). Each table should be titled and typed double-spaced on a separate page. Units must be clearly indicated for each of the entries in the table. Footnotes to tables should be identified by the symbols *,†, ‡, §, ¶ (in that order) and placed at the bottom of the table. No vertical rules should be used. Tables should be prepared in portrait orientation wherever possible.

Figures Figures should be cited consecutively in the text (e.g. Fig. 1, Fig. 2, etc.) and should be grouped together at the end of the paper or in a separate file(s). Legends should be grouped at the end of the paper. Line figures and combination figures should preferably be submitted in vector graphics format (e.g. PDF or EPS format, or embedded as vector graphics in a Word or PowerPoint document). If this is not possible, they should be saved separately as pixel-based graphics at 600 d.p.i. at the required print size, and they should be created and saved in tif (not jpg) format. Note that vector graphics are the preferred format for line and combination figures because figure quality can then be maximized in the online PDF publication. Photographic figures (photos) should be saved at 300 d.p.i. in jpg or tif format. Figures should be created at their smallest practicable size to fit either a single column (max. width 80 mm), two-thirds page width (max. width 110 mm), or a double column (max. width 166 mm). Over-sized figures will be reduced for publication. If figures are created larger than intended publication size, component parts such as symbols and text must be large enough to allow for the necessary reduction. For full instructions on preparing your figures, see http://authorservices.wiley.com/bauthor/illustration.asp.

Scientific names Provide the Latin names of each species in full, together with the authority for its name, at first mention in the main text. If there are many species, cite a flora or checklist that may be consulted for authorities instead of listing them in the text. Do not give authorities for species cited from published references. Give priority to scientific names in the text (with colloquial names in parentheses if desired).

Units and symbols Authors are requested to use the International System of Units (SI, Systme International d'Unités) where possible for all measurements (see *Quantities, Units and Symbols*, 2nd edn., 1975, The Royal Society, London). Note that mathematical expressions should contain symbols not abbreviations. If the paper contains many symbols, it is recommended that they should be defined as early in the text as possible, or within a subsection of the Materials and Methods section.

Supporting Information Supporting Information can be published online at the Editors' discretion. This may include information on, for example, sampling locations, data underlying analyses or figures, additional analyses not presented in the manuscript, or relevant multimedia files (e.g. mating song audio clips). Supporting Information must be formatted and supplied by the author in a ready-to-publish form (wide line spacing and line numbering is therefore not required). Please label Supporting Information S1, S2, S3, etc., for example Appendix S1, Appendix S2, Figure S1, Movie S1. Please compose the Supporting Information section at the end of your article using shortened titles of the Supporting Information if the full titles are long (more than a short sentence). Full titles should be supplied with the Supporting Information itself and will be published online. Further guidelines for authors are available at: http://authorservices.wiley.com/bauthor/suppinfo.asp.

Statistical results In-line statistical results should be presented with the test-statistic followed by degrees of freedom as subscript(s) to the test-statistic (e.g. $F_{1,12} = 1.74$, $P \leq 0.001$). Depending on the details of the analyses, results reported may include parameter estimates, test-statistics, degrees of freedom, significance levels and error/residual model information (e.g. error MS and d.f. in ANOVA or regression models). Since exact P-values can be useful for meta-analyses, we ask that these are quoted even when non-significant, e.g. $t_{23} = 0.25$, $P = 0.34$. However, nonsignificant tests (i.e. $P > 0.05$) should always be interpreted as such.

Cover image

Authors who have their paper accepted for publication are encouraged to submit a photograph(s) illustrating their work (please do not submit photographs until your paper has been accepted). These should be of publishable quality, both in terms of content and image quality. They should be approximately 300 d.p.i. when sized to 15 cm height (max.) by 21.2 cm width (fixed), and if saved in jpg format a low compression setting should be used. Please crop image to these stated dimensions if possible. Resolutions below about 200 d.p.i. will generally not be of high enough quality for publication. You can email your images to the journal Production Editor at jeb@wiley.com with a brief caption (20 to 40 words). This should include a photo credit. If photographs are not the author's, permission for use must have been obtained prior to submission. The photographer of any cover image published will be required to sign a release form.

Colour figures

Colour photographs or other figures are reproduced online free of charge. Authors are encouraged to make good use of colour wherever possible.

Proofs

Authors will be sent an e-mail alerting them that their PDF proof is available for download. Instructions on annotating the proof using Acrobat's PDF annotation tools and uploading corrections to the Wiley Online Proofing server will be included. Authors should complete their proof review within 48 hours of receipt.

Offprints

Free access to the final PDF offprint or your article will be available via Author Services only. Please therefore sign up for Author Services when your paper is accepted if you would like to access your article PDF offprint and enjoy the many other benefits that Author Service offers (see above). Paper offprints may also be purchased and should be ordered when you return your proof corrections by following the instructions supplied at the time.

Cover legend: Artist's impression of evolution of specialization in a dynamic fluid. Physical factors such as diffusion, flow patterns, and decay rates are as influential as fitness economics in governing the evolution of community structure. See Uppal et al., (pp. 256–269). Photo Credit: Dervis Can Vural (co-author)

Early View

The *Journal of Evolutionary Biology* is covered by Wiley Blackwell's Early View service. Early View articles are complete full-text articles published online in advance of the publication in a online or printed issue. Articles are therefore available as soon as they are ready, rather than having to wait for the next scheduled issue. Early View articles are complete and final. They have been fully reviewed, revised and edited for publication, and the authors' final corrections have been incorporated. Because they are in final form, no changes can be made after online publication. The nature of Early View articles means that they do not yet have volume, issue or page numbers, so Early View articles cannot be cited in the traditional way. They are therefore given a Digital Object Identifier (DOI), which allows the article to be cited and tracked before it is allocated to an issue. After print publication, the DOI remains valid and can continue to be used to cite and access the article.

Copyright Transfer Agreement

If your paper is accepted, the author identified as the formal corresponding author for the paper will receive an email prompting them to login into Author Services; where via the Wiley Author Licensing Service (WALS) they will be able to complete the license agreement on behalf of all authors on the paper. If the OnlineOpen option is not selected the corresponding author will be presented with the copyright transfer agreement (CTA) to sign.

Online Open

OnlineOpen is available to authors of primary research articles who wish to make their article available to non-subscribers upon publication, or whose funding agency requires grantees to archive the final version of their article. With OnlineOpen the author, the author's funding agency, or the author's institution pays a fee to ensure that the article is made available to non-subscribers upon publication via Wiley Online Library, as well as deposited in the funding agency's preferred archive. The charge for OnlineOpen publication is $3,000 (discounted to $1,500 for papers where the first or corresponding author is a current member of the European Society for Evolutionary Biology, www.eseb.org). For the full list of terms and conditions, see http://wileyonlinelibrary.com/onlineopen#OnlineOpen_Terms.

Any authors wishing to publish their paper Online Open will be required to complete the payment form available on our website at: https://authorservices.wiley.com/bauthor/onlineopen_order.asp. Prior to acceptance there is no requirement to inform an Editorial Office that you intend to publish your paper Online Open if you do not wish to. All Online Open articles are treated in the same way as any other article. They go through the journal's standard peer-review process and will be accepted or rejected based on their own merit.

Free access in the Developing World

Free online access to this journal is available within institutions in the developing world through the HINARI initiative with the World Health Organization (WHO), the AGORA initiative with the Food and Agriculture Organization of the United Nations (FAO) and the OARE Initiative (Online Access to Research in the Environment) with the United Nations Environment Programme (UNEP).

Data Sharing

The *Journal of Evolutionary Biology* requires, as a condition for publication, that data supporting the results in the paper should be archived in an appropriate public archive, such as GenBank, TreeBASE, Dryad, the Knowledge Network for Biocomplexity or other suitable long-term and stable public repositories. Data are important products of the scientific enterprise, and they should be preserved and usable for decades in the future. Authors may elect to have the data publicly available at time of publication, or, if the technology of the archive allows, may opt to embargo access to the data for a period up to a year after publication. Longer embargoes or exceptions to depositing data may be granted at the discretion of the Editor-in-Chief, especially for sensitive information such as human subject data or the location of endangered species. All accepted papers should provide accession numbers or DOI for data underlying the work that have been deposited, so that these can appear in the final accepted article.

Received: 16 October 2019 | Revised: 16 January 2020 | Accepted: 20 January 2020

DOI: 10.1111/jeb.13593

RESEARCH PAPER

JOURNAL OF Evolutionary Biology ESEB WILEY

Evolution of specialized microbial cooperation in dynamic fluids

Gurdip Uppal | Dervis Can Vural

University of Notre Dame, Notre Dame, IN, USA

Correspondence
Dervis Can Vural, University of Notre Dame, 225 Nieuwland Science Hall, 46556 Notre Dame, IN, USA.
Email: dvural@nd.edu

Funding information
Defense Advanced Research Projects Agency, Grant/Award Number: HR0011-16-C-0062; National Science Foundation, Grant/Award Number: CBET-1805157

Abstract

Here, we study the evolution of specialization using realistic computer simulations of bacteria that secrete two public goods in a dynamic fluid. Through this first-principles approach, we find physical factors such as diffusion, flow patterns and decay rates are as influential as fitness economics in governing the evolution of community structure, to the extent that when mechanical factors are taken into account, (a) generalist communities can resist becoming specialists despite the invasion fitness of specialization; (b) generalist and specialists can both resist cheaters despite the invasion fitness of free-riding; and (c) multiple community structures can coexist despite the opposing force of competitive exclusion. Our results emphasize the role of spatial assortment and physical forces on niche partitioning and the evolution of diverse community structures.

KEYWORDS

evolution of co-operation, microbes, natural selection, population genetics, simulation, theory, trade-offs

1 | INTRODUCTION

From subcellular structures to ecological communities, life is organized in compartments and modules performing specific tasks. Organelles (Kutschera & Niklas, 2005; Siegel, 1960), single (Lewis, 2007) and multi-phenotype (Fu et al., 2018; Koufopanou, 1994) bacterial populations, tissues and organs in multicellular organisms (Carroll, 2001; Hedges, Blair, Venturi, & Shoe, 2004), casts and social classes in colonial animals (Beshers & Fewell, 2001; Smith, Toth, Suarez, & Robinson, 2008), and guilds in ecological communities (Futuyma & Moreno, 1988; May & Seger, 1986; Terborgh, 1986), all fulfil specialized roles that are vital for the functioning of a larger whole. Specialization also gives rise to metabolic interdependencies in microbial populations and can serve as a strong mechanism for community assembly (Zelezniak et al., 2015).

Evolution of specialization is typically studied in terms of fitness trade-offs or economic considerations. Specialization emerges if relatedness is high and if fitness returns accelerate (Michod, 2007; Michod, Viossat, Solari, Hurand, & Nedelcu, 2006; Rueffler, Hermisson, & Wagner, 2012; Tannenbaum, 2007; Taylor, 1992; Vural, Isakov, & Mahadevan, 2015; Willensdorfer, 2009). There are two classes of evolutionary forces moving a population from having one type of individual performing multiple functions –generalism–, towards one that has multiple types of individuals performing distinct functions –specialism–. The first is 'incompatible optimas' (Goldsby, Dornhaus, Kerr, & Ofria, 2012; Solari, Kessler, & Goldstein, 2013; Sriswasdi, Yang, & Iwasaki, 2017): if a population must optimize two functions at once, but the phenotypes optimizing these are incompatible, then the population will split into two phenotypes. For example, the somatic and germ cells in volvox colonies are optimized for motility and reproduction. As a result, they have entirely different positioning (Solari, Kessler, & Michod, 2006), morphology (Kirk, 2001), and protein expression (Kirk & Kirk, 1983). In multicellular cyanobacteria, cells differentiate into carbon-fixating cells and nitrogen-fixating heterocysts (Rossetti, Schirrmeister, Bernasconi, & Bagheri, 2010). *E. coli* can differentiate into transient

The peer review history for this article is available at https://publons.com/publon/10.1111/jeb.13593

nongrowing cells and normally growing cells to hedge their bets across different environments (Lewis, 2007). A travelling band of *E. coli* will exhibit a continuum of navigation styles, each specializing in processing different local conditions while still moving in unison (Fu et al., 2018).

A second type of evolutionary pressure originates from the economies of scale. Undertaking one process at high volume is more cost-effective than undertaking multiple processes at low volume. The morphological characteristics necessary to accomplish two distinct functions require two investments in overhead. Specialization is then favoured if fitness returns are accelerated by further investment into a specific task (Cooper & West, 2018; West, Fisher, Gardner, & Kiers, 2015).

It is well known that spatial structure is key in the evolution of cooperation (Durrett & Levin, 1994; Lion & Baalen, 2008; Taylor, 1992; Uppal & Vural, 2018; Wakano, Nowak, & Hauert, 2009). By forming fragmenting groups, multicellular organisms and social colonies can combat fixation of cheaters. Coexistence of cheaters and cooperators is also enhanced in spatially structured populations (Wilson, Morris, & Bronstein, 2003). Understanding how spatial structuring arises and competition within and across groups can shed light on how cooperation and resistance to cheaters arise (Lion & Baalen, 2008). Here, we will be interested in the role of spatial structuring in the evolution of specialization.

Existing computational models of evolution of specialization that consider spatial structure or finite group size typically abstract away the underlying physics (Cooper & West, 2018; Gavrilets, 2010; Ispolatov, Ackermann, & Doebeli, 2012; Menon & Korolev, 2015; Oliveira, Niehus, & Foster, 2014; Rueffler et al., 2012; Schiessl et al., 2019; Vural et al., 2015; Willensdorfer, 2008). While conceptually useful, such models reveal little about the interplay between evolutionary and mechanical forces during the formation and evolution of specialization. Real-life microbial exchanges are mediated almost entirely by viscoelastic secretions that diffuse and flow (West, Diggle, Buckling, Gardner, & Griffin, 2007). Extracellular enzymes digest food (Bachmann, Molenaar, Kleerebezem, & Hylckama Vlieg, 2011; Greig & Travisano, 2004; Pirhonen, Flego, Heikinheimo, & Palva, 1993), surfactants aid motility (Kearns, 2010; Xavier, Kim, & Foster, 2011), chelators scavenge metals (Griffin, West, & Buckling, 2004; Guerinot, 1994; Harrison & Buckling, 2009; Kümmerli, 2010; Neilands, 1984; Ratledge & Dover, 2000), toxins fight competitors and antagonists (An, Danhorn, Fuqua, & Parsek, 2006; Inglis, Gardner, Cornelis, & Buckling, 2009; Mazzola, Cook, Thomashow, Weller, & Pierson, 1992; Moons et al., 2006; Moons, Van Houdt, Aertsen, Vanoirbeek, & Michiels, 2005), virulence factors exploit a host (Allen, McNally, Popat, & Brown, 2016; Kohler, Buckling, & Delden, 2009; Sandoz, Mitzimberg, & Schuster, 2007; Zhu et al., 2002), and extracellular polymeric substances provide sheltering (Davies, 2003; Mah & O'toole, 2001; Xue, Sendamangalam, Gruden, & Seo, 2012). Since cells must be within a certain distance to exchange such services, spatial aggregation is considered a prerequisite for multicellular specialization. Spatial effects matter (Durrett & Levin, 1994; Fletcher & Doebeli, 2009; McNally et al., 2017;

Specialization

Large waste diffusion: Larger waste diffusion lowers self-competition and allows specialists to form denser groups to better utilize public goods secreted by neighbours.
Large public good benefit: A high benefit for public goods allows specialists to still be fit without secreting as many public goods. This also helps cheaters exploit producers.
Lower secretion costs: A lower secretion cost can help specialists dominate over generalists, since a smaller penalty for cooperation can make generalists groups too large and more vulnerable to specialist mutations. In this case, large generalist structures are easily taken over by specialist mutants.
Group structure: Specialists form groups when waste diffusion is larger than public good diffusion and when costs are not too low. When specialists do not form groups, they are easily taken over with cheaters, leading to either 'chasing cheaters', (Video S6), or extinction. When generalists form smaller, fragmenting groups, they are able to escape takeover by specialists and out-compete specialists.
Fitness type: The fitness type dictates which types of specialist structure we see—pure or mixed. In the OR case, specialists generally evolve into structures of isolated types of specialists (Video S4). The AND structure is therefore essential to have true division of labour, where each type of specialist exists equally in the group (Video S3).

Cheater coexistence

Lack of group structure and small invasion fitness: Cheaters cannot exist on their own, but must 'predate' on producers—generalists or specialists. When producers are fit, and do not form groups, they can grow quicker than cheaters fully taking over. This occurs when waste diffusion is large, and when secretion costs are low. Low secretion cost also lowers the invasion fitness of cheaters, since the advantage of not secreting is lower, helping them to coexist (Video S6).

Extinction

When cheaters take over: Cheaters take over when their invasion fitness is large and mutation rates are faster than group fragmentation rates. This occurs when public good benefit is large and/or when waste diffusion is large, as seen in top-middle regions of plots given in Figure 5.
When groups are not stable: When costs are large and public good benefit is low, cooperators need to form denser groups to increase fitness. However, with low waste diffusion, denser groups over-pollute themselves and are no longer stable. We see this in the bottom-right regions of plots in Figure 5.

Fluid shear

Enhanced group fragmentation: A shearing flow stretches and distorts groups. It can help groups fragment and reproduce quicker, allowing stability over cheating mutations (Uppal & Vural, 2018).

Enhanced specialization in linear and vortex flows: Shearing flow can help specialist groups fragment quicker than generalist groups and therefore transition a population to contain more specialists (Figure 4c,d, Video S2).

Coexistence of group types: The local shear rate can determine what groups are stable. A spatially varying flow profile can then allow for coexistence of different community structures across the full fluid domain (Figure 6, Videos S7 and S8).

Wakano et al., 2009; Wilson et al., 2003), and multiple factors can couple together to influence the evolution of cooperation (Dobay, Bagheri, Messina, Kümmerli, & Rankin, 2014) and division of labour (Dragoš et al., 2018) in unexpected ways.

In this study, we find that mechanical factors such as diffusion constants, molecular decay rates and fluid flow patterns play a crucial role in shaping the interaction structure of an ecological community. We find, through first-principles computer simulations and matching analytical formulas, that microbes self-aggregate and form evolving clusters, whose size, shape and economical exchanges are sensitively dependent on the physical parameters defining the abiotic environment. Such structures have already been empirically observed in *E. coli* (Budrene & Berg, 1991), *S. typhimurium* (Blat & Eisenbach, 1995), and *B. subtilis* (Mendelson & Lega, 1998) (Figure 1) and studied theoretically (McNally et al., 2017; Stump, Johnson, & Klausmeier, 2018; Tsimring et al., 1995; Wakano et al., 2009). However, the interplay between evolutionary and mechanical forces within and between these structures and their role in the formation and evolution of community interactions remain unknown.

Since many bacterial products leak outside the cell, members of the local community can exploit their neighbours and evolve to delete costly functions. The Black Queen Hypothesis suggests that loss of functionality occurs due to selfish mutations and can form the basis for mutualistic relationships (Morris, Lenski, & Zinser, 2012; Sachs & Hollowell, 2012). Thus, from evolutionary game theoretical considerations alone, one expects that specialists always eventually dominate a population of generalists. How then should we explain the persistence of generalists in nature, and even the coexistence of various combinations of generalists, specialists, and cheaters within one niche?

To address this question, we construct a mechanistic model that naturally gives rise to distinct microbial clusters. We then analyse the evolutionary transitions between generalized and specialized interactions within clusters for different fluid flow patterns, diffusion lengths, molecular decay constants and cell growth kinetics. Lastly, we study the competitive interactions across clusters.

In doing so, we establish the physical factors that counteract game theoretical expectations, that is factors that allow generalists to resist specialization, and generalists and specialists to resist cheaters. We also establish physical factors that counteract competitive exclusion, that is allowing multiple community types to coexist within the same fluid niche. Lastly, we determine what physical properties make 'socially uninhabitable' niches, where free-riders emerge, exploit and invariably destroy both generalist and specialist communities.

2 | METHODS

Any model aiming to describe evolution of functional specialization must include at least two functions, so that subpopulations can potentially specialize to perform one function each. In our model, microbes can secrete two public goods and a waste/toxin. These molecules diffuse, flow and decay (cf. Figure 2).

The specific assumptions of our model, qualitatively stated, can be enumerated as follows: (1) the system consists of microbes that can secrete two kinds of public goods. A public good refers to a secretion that promotes the growth of nearby microbes (including the producer). The producer also pays a metabolic cost for secreting the public good. (2) Every microbe secretes a waste molecule that curbs the growth of those nearby. (3) The secretions and bacteria obey the physical laws of fluid dynamics and diffusion. (4) Whether a microbe secretes both, one or none of the public goods is hereditary, except for mutations. However, every phenotype emits waste.

We study two models separately. (5) In one, which we call AND, access to both kinds of goods is necessary. In the other, which we call OR, both goods contribute to fitness, but the lack of one can be compensated with the other.

Our work consists of discrete, stochastic agent-based simulations and related continuous deterministic equations. In addition, to gain better analytical understanding, we construct a simple effective model that captures the essential outcomes of the simulations.

2.1 | Continuous deterministic equations

We construct equations governing the number density of four phenotypes $n_0(x,t)$, $n_1(x,t)$, $n_2(x,t)$, $n_3(x,t)$ two chemical secretions that are public goods $c_1(x,t)$, $c_2(x,t)$, and a waste compound $c_3(x,t)$, as a function of space x and time t. $n_3(x,t)$ is the number density of microbes that secrete both kinds of public goods, to which we refer as 'generalists'. The microbes that secrete only public good one or two are denoted by $n_1(x,t)$ and $n_2(x,t)$, to which we refer as 'specialists'. Those that secrete no public goods are denoted by $n_0(x,t)$, to which we refer as 'cheaters'.

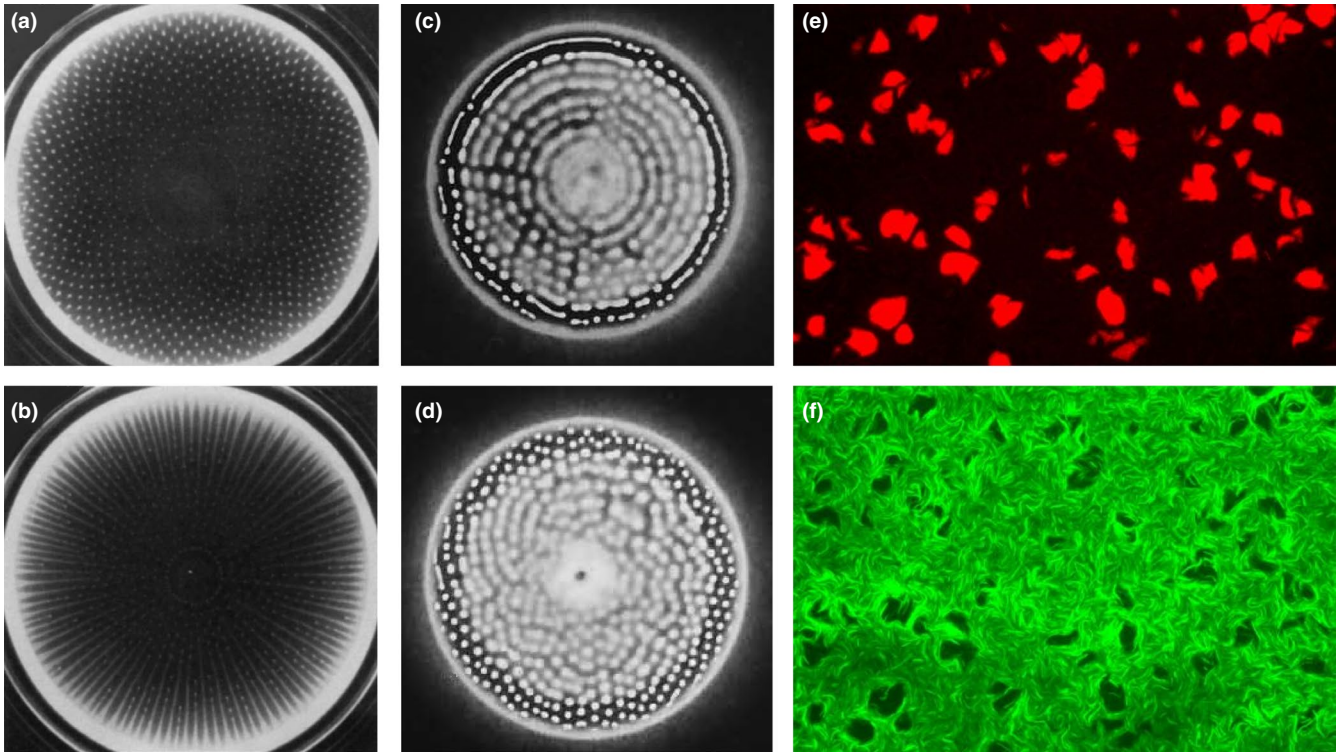

FIGURE 1 Pattern-forming populations. (a, b) Examples of spatial patterning of bacteria in experiments performed by Budrene and Berg (1991). *E. coli* formed spots (a) and stripes (b) in response to public goods they themselves excrete. (c, d) Aggregation patterns observed in *S. typhimurium* in experiments by Blat and Eisenbach (1995). (e, f) Spot (e) and hole (f) patterns observed in experiments with synthetic bacteria performed by Karig et al. (2018). Figures courtesy of authors

$$\dot{n}_i = \left(d_b \nabla^2 - v(x,t)\cdot\nabla + f_i(c)\right) n_i + \sum_{j=0}^{3} M_{ij} n_j \tag{1}$$

$$\dot{c}_\alpha = \left(d_\alpha \nabla^2 - v(x,t)\cdot\nabla - \lambda_\alpha\right) c_\alpha + \sum_{i=0}^{3} S_{i\alpha} n_i \tag{2}$$

Here, indices $i, j = 0, 1, 2, 3$ label phenotypes, whereas the index $\alpha = 1, 2, 3$ labels chemicals, that is the two public goods and waste. Thus, Equations (1) and (2) comprise 7 coupled spatiotemporal equations.

In both equations, the first two terms describe diffusion and advection. The flow field $\mathbf{v}(x,t)$ is a vector-valued function of space and time and includes all information pertaining the flow patterns in the environment. In general, it is obtained by solving separate fluid dynamics equations. Mutations and secretions are governed by two matrices,

$$M = \mu \begin{bmatrix} -2 & 1 & 1 & 0 \\ 1 & -2 & 0 & 1 \\ 1 & 0 & -2 & 1 \\ 0 & 1 & 1 & -2 \end{bmatrix}, \quad S = \begin{bmatrix} 0 & 0 & s_w \\ s_1 & 0 & s_w \\ 0 & s_2 & s_w \\ s_1 & s_2 & s_w \end{bmatrix}.$$

The secretion rate of chemical α by phenotype *i* is given by the matrix element $S_{i\alpha}$, and its decay rate by λ_α. The mutation rate from phenotype *j* to *i* is given by M_{ij}. The diagonal elements M_{ii} indicate the rate at which *i* mutates to become something else.

Note that in our model, the secretion of public goods is binary, that is a good is either secreted or not. Mutations toggle on and off with probability μ whether an individual secretes either public good. A mutation can cause a generalist to become a specialist, but two mutations, one for each secretion function, are required for a generalist to become a cheater. Same with back mutations.

The fitness function $f_i(\mathbf{c})$ determines the growth rate of phenotype *i*. We consider two cases separately: when both public goods are necessary for growth (AND) and when the public goods can substitute one-to-one for one other (OR).

$$f_i^{(\mathrm{AND})} = a_{12}\frac{c_1 c_2}{c_1 c_2 + k_{12}} - a_w \frac{c_3}{c_3 + k_w} - \sum_{\alpha=1}^{2} \beta_\alpha S_{i\alpha} \tag{3}$$

$$f_i^{(\mathrm{OR})} = a_{12}\frac{(c_1 + c_2)}{(c_1 + c_2) + k_{12}} - a_w \frac{c_3}{c_3 + k_w} - \sum_{\alpha=1}^{2} \beta_\alpha S_{i\alpha} \tag{4}$$

As we see, in both cases, growth rate increases with the local concentration of public goods, c_1, c_2 and decreases with the concentration of waste, c_3. β_α is the cost of secreting public good α, so that growth of phenotype *i* is curbed by an amount proportional to its public good secretion. Waste is produced without any cost.

Note that with increasing concentration of goods, microbes receive diminishing returns. Similarly, with larger waste, death rate approaches a maximum value. These functional forms are well understood, experimentally verified (Monod, 1949), and commonly

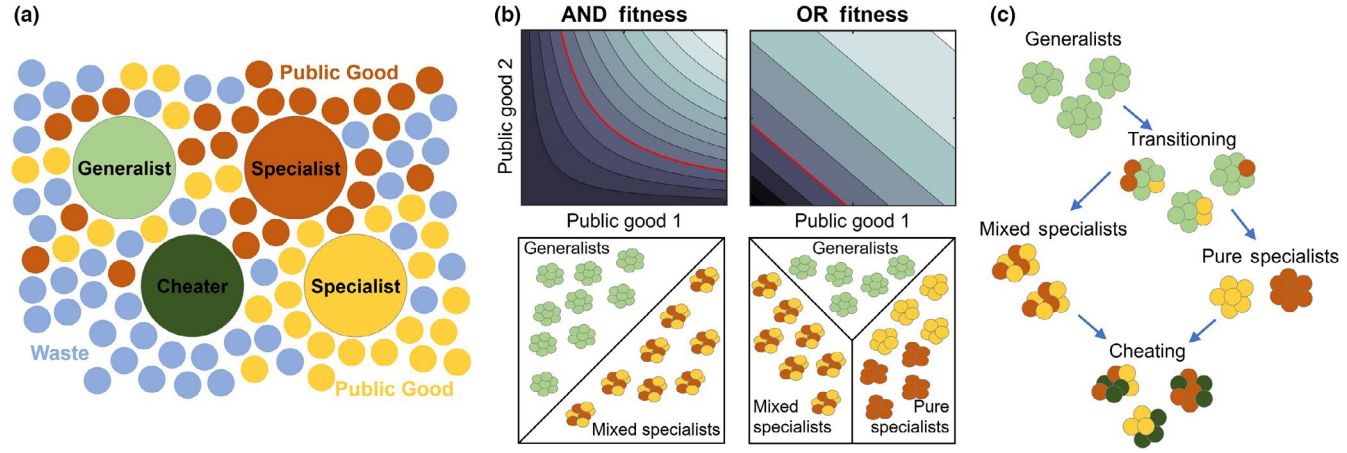

FIGURE 2 Schematics and dynamics of the model. (a) Microbes cooperate by secreting public goods into their environment. Generalists (large green circles) secrete two public goods (small yellow and red circles). Specialists (large red and yellow circles) secrete only one of the two public goods. Cheaters (dark green) secrete none of the public goods. All microbes secrete a metabolic waste (small blue circles). (b) Fitness contour plots and types of stable groups in each fitness variant. In the top row, we plot the fitness contours as a function of public good concentrations c_1 and c_2. In the bottom row, we show the types of stable groups in each fitness form. The red line represents the contour corresponding to zero fitness. In the AND case, the red line can never cross the c_1, c_2 axes, and the fitness is negative when either chemical is not present. Therefore, the only types of stable groups are generalists or mixed specialists, as shown in the bottom-left panel. In the OR case, the contours form straight lines. A decrease in one chemical is equally compensated by an increase in the other chemical. The zero contour always crosses the c_1, c_2 axes. It is therefore also possible to have pure specialist groups in the OR case, as shown in the bottom-right panel. (c) Evolutionary paths between group types. Groups typically move towards less secretion since cheaters have higher invasion fitness than specialists, who, being 'half-cheaters', have higher invasion fitness than generalists

used in population dynamics models (Allen & Waclaw, 2018). *a*'s and *k*'s are constants defining the initial slope and saturation values of growth and death (see Table 1).

2.2 | Discrete stochastic simulations

Our analytical conclusions (cf. Section S1) have been guided and supplemented by agent-based stochastic simulations in two dimensions. Videos of these simulations are provided in Supplementary Videos. Our simulation algorithm is as follows: at each time interval, Δt, the microbes (1) diffuse by a random walk of step size $\delta = \sqrt{4d_b \Delta t} + \vec{v}\Delta t$ derived from the diffusion constant plus a bias dependent on the flow velocity. (2) Microbes secrete chemicals locally onto a discrete grid that then diffuse using a finite difference scheme. (3) Microbes reproduce or die with a probability dependent on their local fitness and time step, given by $f(\mathbf{c})\Delta t$. If $f\Delta t$ is negative, the microbes die with probability 1, and if $f\Delta t$ is between 0 and 1, they reproduce an identical offspring with probability $f\Delta t$. Upon reproduction, offspring are placed at the same location as their parent. (4) Random mutations may alter the secretion rate of either public good—and thus the reproduction rate—of the microbes. Mutations occur on each secretion function with probability μ and turn the secretion of the public good on or off. The secretion rate is assumed to be heritable and constant in time. Numerical simulations for figures were performed by implementing the model described above using the Matlab programming language and simulated using Matlab (Mathworks, Inc.). The source code for discrete simulations is provided as a supplemental file. Additional details of model implementation are discussed in Section S2.

A summary of the system parameters is given in Table 1, along with typical ranges for their values used in the simulations. Parameter values as well as the simulation domain (the physical region being simulated) are also given in figure captions. The relevant ratios of parameters are consistent with those observed experimentally (Drake, Charlesworth, Charlesworth, & Crow, 1998; Gibson, Wilson, Feil, & Eyre-Walker, 2018; Kim, 1996; Ma, Zhu, Ma, & Yu, 2005; Rusconi & Stocker, 2015). Note also that the choice of parameters will be restricted to ensure a finite stable solution is possible. For example, we enforce the quantity $a_{12} - a_w - \beta_1 s_1 - \beta_2 s_2 < 0$. This is because, if this quantity was positive, then a dense population, where the Hill terms in the fitness functions are saturated, will continue to have a positive fitness and grow indefinitely. In the case where secretion rate and/or production costs are low, the waste term is crucial to ensure a finite carrying capacity. We therefore choose $a_w \geq a_{12}$. Other constraints on existence and stability are derived in our Turing analysis (see Section S1). Further discussion on parameter selection and sensitivity is also given in Section S2.

2.3 | Simple effective model

To gain better analytical understanding, we set to reproduce the outcomes our complex model with a much simpler effective model, which we describe in Section S3. Our effective model is based on the observation that microbes aggregate into self-reproducing

TABLE 1 Summary of system parameters

	Quantity	Values for OR	Values for AND
d_b	Microbial diffusion	0.4×10^{-4} cm^2/s	1×10^{-6} cm^2/s
d_1	Good 1 diffusion	5 and 25×10^{-6} cm^2/s	5 and 20×10^{-6} cm^2/s
d_2	Good 2 diffusion	5 and 25×10^{-6} cm^2/s	5 and 20×10^{-6} cm^2/s
d_w	Waste diffusion	$10–80 \times 10^{-6}$ cm^2/s	$10–80 \times 10^{-6}$ cm^2/s
λ_1	Good 1 decay	5.0×10^{-3} s^{-1}	5.0×10^{-3} s^{-1}
λ_2	Good 2 decay	5.0×10^{-3} s^{-1}	5.0×10^{-3} s^{-1}
λ_w	Waste decay	1.5×10^{-3} s^{-1}	1.5×10^{-3} s^{-1}
k_{12}	Goods saturation	0.01	3×10^{-5}
k_w	Waste saturation	0.1	0.1
s_1	Good 1 secretion rate	5.0×10^{-3} s^{-1}	0.01 s^{-1}
s_2	Good 2 secretion rate	5.0×10^{-3} s^{-1}	0.01 s^{-1}
s_w	Waste secretion rate	0.01 s^{-1}	0.09 s^{-1}
a_{12}	Benefit from goods	$62.5–80 \times 10^{-3}$ s^{-1}	$40–75 \times 10^{-3}$ s^{-1}
a_w	Harm from waste	8.0×10^{-3} s^{-1}	10.5×10^{-3} s^{-1}
β_1	Cost of good 1	0.01–0.26	0.01–0.15
β_2	Cost of good 2	0.01–0.26	0.01–0.15
μ	Mutation rate	5.0×10^{-8} s^{-1}	2.0×10^{-7} s^{-1}

cooperative groups. Different group types, rather than individual microbes, constitute the basic building blocks of our effective model, and the fragmentation rates of these group types constitute the basic parameters of the model. These parameters are 'measured' from our complex simulations and depend on the physical properties of the system (see Figures S2 and S3). The results of our effective model are compared to simulation results in Figure 4.

3 | RESULTS

3.1 | Cooperative groups as Turing patterns

Through numerical simulations and analytical formulas, we see that the system gives rise to spatially segregated cooperating groups in a certain parameter range, as shown in Figure 3. Spots or stripes in reaction diffusion systems are known as Turing patterns, which form whenever an inhibiting agent diffuses faster than an activating agent. In our model, the inhibiting and activating agents are the waste and the public goods.

In general, the structure and size of these cooperating groups will vary with physical parameters. We show in Figure 3 how the Turing pattern-forming region varies with diffusion constants, in the absence of mutations or flow. Our analytical result, derived in Section S1, shown by the thick blue lines, delineates the parameter space into pattern-forming and non-pattern-forming regions. While simulations agree well with analytical results, we see some patterns slightly beyond the theoretical region. This is due to the stochastic nature of the simulations which is known to widen the pattern-forming region (Biancalani, Fanelli, & Di Patti, 2010; Butler & Goldenfeld, 2009).

In our simulations, we observe that cooperative groups of microbes, that is spots and stripes, grow and fragment, thereby giving rise to new structures of the same type. The spatial structure of these patterns differs between generalists and specialists and therefore has a strong effect on the evolutionary trajectory of the system.

3.2 | Effects of secretion cost on specialization

We next determine the role of secretion cost β_α on group structure and hence specialization, in the absence of flow. To see the effect of trade-offs on specialization, we varied the cost of public good secretion and determined when specialization occurs in both AND and OR fitness forms. To simplify our analysis, we set $s_1 = s_2 = s$. In order for both types of specialists to then coexist, we also set $\beta_1 = \beta_2 = \beta$. Therefore, generalists pay an overall cost of 2β, specialists pay β, and cheaters pay no cost. As such, a specialist mutant will invade a generalist group, and a cheater mutant will invade a specialist group. In the absence of spatial structure and flow, the entire population will be dominated by cheaters and will go extinct.

What can we say about the competition between different group types (as opposed to between different strains within a group)? Since with all else equal, increasing costs harm generalists twice as much as specialists, one might expect that increasing the cost of the goods would favour the specialists over generalists. Counterintuitively, we find the opposite. Specialist groups indeed grow faster and form larger, expansive and denser groups, which however are at once taken over by cheaters. In contrast, generalists form smaller, sparser and weaker groups that fragment more often, which limits the spread of mutants (see Figures S2 and S3). Therefore, at higher cost β, the 'weak' generalists are able to coexist and even dominate 'strong' specialists (Figure 4a,b).

In general, a large uniform population is more susceptible to invading mutants. In contrast, when the population is organized as fragmenting patches, the community structure will prevail as long as the fragmentation rate is larger than the invasive mutation rate. Thus, the type, size, growth and fragmentation of the groups ultimately dictate whether generalism, specialism or a coexistence of group types is evolutionarily stable.

3.3 | Effect of flow patterns on specialization

Fluid dynamical forces can strongly influence the eco-evolutionary dynamics of a microbial population. For example, fluid flows can shape the competition and matrix secretion in biofilms (Nadell, Ricaurte, Yan, Drescher, & Bassler, 2017). A shearing fluid flow has also been shown to modify social behaviour by enhancing

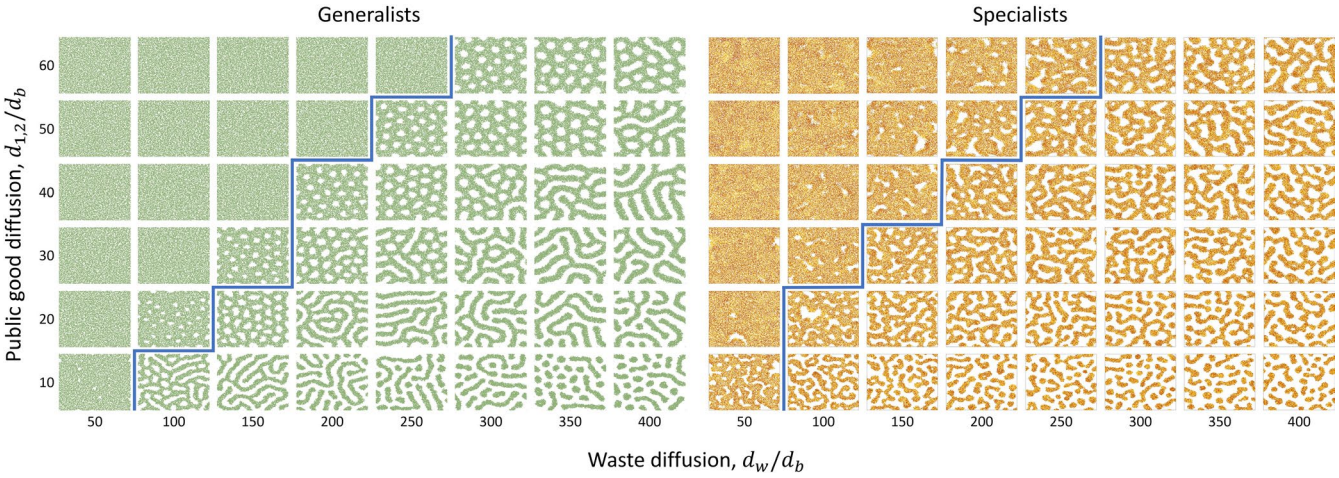

FIGURE 3 Pattern formation in bacteria. In both AND and OR fitness types, microbes can form clusters. We set both the mutation rate and fluid flow rate to zero to study pattern formation in generalist and specialist microbes without additional physical and evolutionary complications. While this figure only shows generalists and specialists subject to AND-type fitness, we observe qualitatively identical patterns for the OR-type fitness. The thick blue line is the result of our analytical calculation indicating the regime where patterns emerge, which agrees with computer simulations (see Section S1). The population can be homogeneous or form stripes or spots. These patterns can also grow and fragment, forming new colonies. The diffusion constants are normalized by the bacterial diffusion constant, $d_b = 1 \times 10^{-6}$ cm^2/s. Secretion constants used are $s_1 = s_2 = 0.015$ s^{-1} and $s_w = 0.005$ s^{-1}, and public good cost is $\beta_1 = \beta_2 = 0.1$. The rest of the parameters are as given in Table 1

the group size and fragmentation rate (Uppal & Vural, 2018). We therefore expect that the flow patterns will affect the mode of cooperation (specialist vs. generalist) and the physical structure of groups.

For constant shear, we used a planar Couette flow, with velocity profile and shear rate given as,

$$\mathbf{v} = v_{\max}\frac{y}{H}\hat{\mathbf{x}}, \quad \left|\frac{dv}{dy}\right| = \frac{v_{\max}}{H},$$

where $v_{\max}$ is the maximum flow rate and H is the height of the domain. Flow is along the $\hat{x}$ direction and is zero in the centre $y = 0$, and maximal at the boundaries $y = \pm H$. We used periodic boundary conditions along the left and right walls ($\hat{\mathbf{x}}$ direction), and Neumann boundary conditions for the top and bottom surfaces ($\hat{\mathbf{y}}$ direction).

The effect of shear is in general nontrivial and will depend on the group structure observed. We find that a shearing flow increases group fragmentation rate of microbes organized in distinct circular spots, whereas it simply enlarges groups when they are organized in an elongated, stripe-like fashion.

In Figure 4c,d, we show the effect of shear at intermediate costs, where its effect is strongest. We found in both cases that larger shear helps specialists by enhancing their fragmentation rate and enlarging generalist groups (Figures S2 and S3), since larger generalists groups generate more mutations, and since faster fragmenting specialist groups are better able to resist takeover by cheaters. Here, fluid shear transitions the system from a generalist or coexisting state to a specialist state (Video S2). Thus, fluid shear promotes specialization.

Since advective flow is something that one can tune in an experimental or industrial setting, it is exciting to think of possibilities where flow is used to control the social evolution of a microbial community. Furthermore, since shear is in general spatially dependent, we can use different velocity profiles to localize this control to different regions.

3.4 | Effect of public good benefit, cooperation cost and competition on evolution of specialization

We next study how varying public good benefit, production cost and waste diffusion affect the stability of different community structures (Figure 5). We find that higher waste diffusion and public good benefit help specialists and higher secretion cost favours generalists. Figure 5 also shows what conditions lead to coexistence of different group types.

If waste diffusion is large, self-competition is lower, and specialists can form denser groups without over-polluting themselves (top regions in Figure 5a,b). They can then better utilize public goods secreted by their neighbours. If the public good benefit, a_{12}, is large, specialists also do better since secreting fewer public goods still gives a large benefit (top regions in Figure 5c,d, see also Video S3 for AND fitness variant and Video S4 for OR fitness).

As we have already seen, specialization emerges when trade-offs are small, that is at smaller β. At higher β, generalists are able to coexist with specialists (see Figure 5g and Video S5 for OR fitness) and constitute the majority of the population (Figure 5e and Video S1).

We also see that cheaters can persist stably with the population when their invasion fitness is lower than the growth rate of producers. This occurs in regions where producers do not form groups but grow either as stripes or homogeneously in space, which happens when public good benefit is large and when secretion

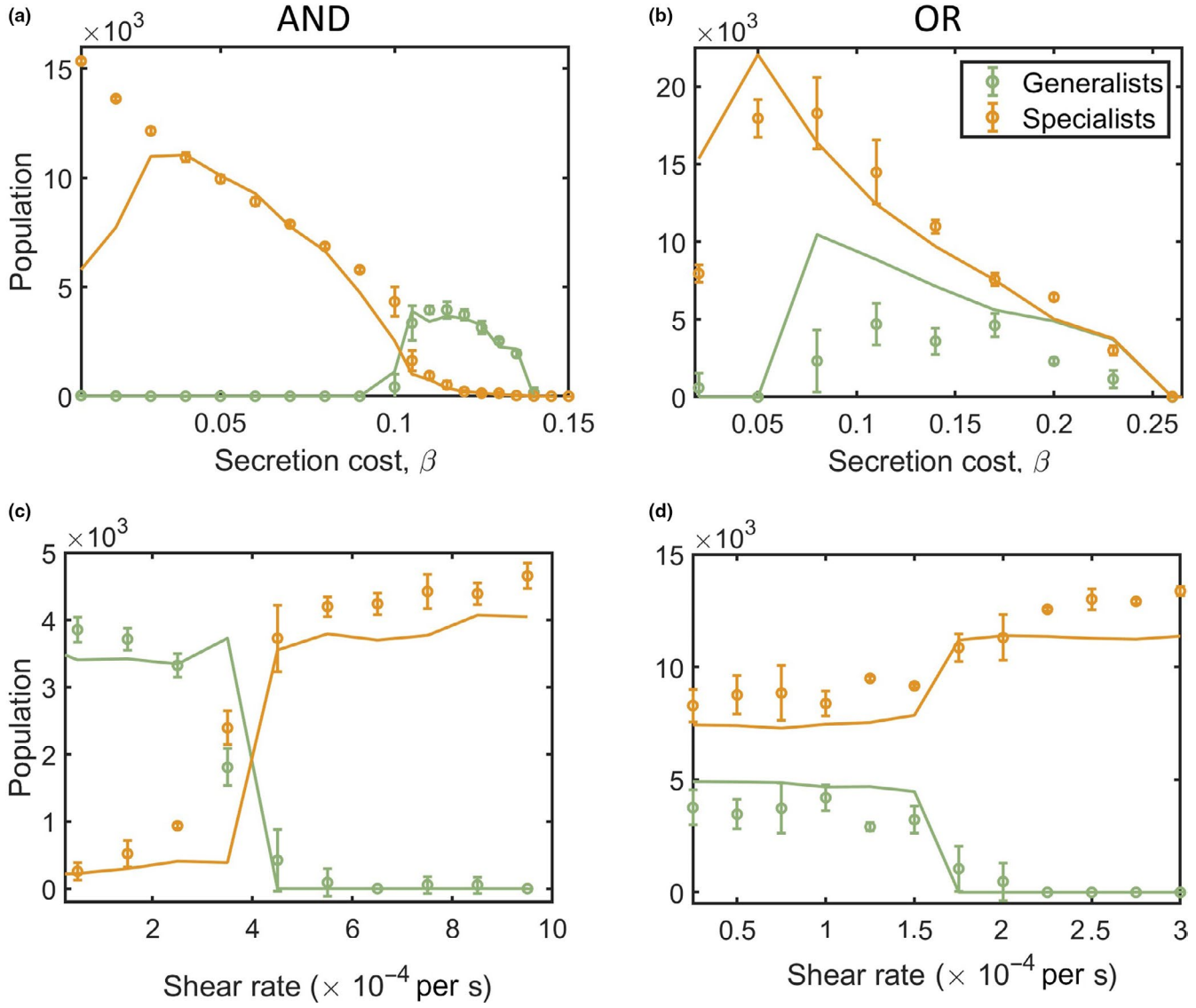

FIGURE 4 Effects of cooperation cost and fluid shear on specialization. Points with error bars represent numerical results averaged over 5 runs at simulation time $T = 2 \times 10^6$ S in a domain of size 20 mm × 20 mm. Error bars correspond to one standard deviation from the mean. Solid lines are from our effective theoretical model given in Section S3. (a, b) Effects of secretion costs in the absence of flow. In each fitness variant, we see that specialization is more abundant for low costs. At lower costs, generalist groups are 'too fit' and form large aggregate structures that are more susceptible to mutations. At higher costs, a, we see generalists out-compete specialists, in the AND case (see Video S1) and b, coexist with specialists in the OR case (Video S5). At low costs, specialists again dominate. (c, d) Effects of fluid shear. A shearing flow causes groups to fragment quicker and stripes to elongate and grow larger. (c) In the AND case, with secretion cost $\beta = 0.12$, we observe that shear transitions the system from a coexisting state to a specialist state (see Video S2). Here, shear causes generalists groups to elongate and become more susceptible to mutations. (d) In the OR case, at cost $\beta = 0.17$, shear again causes a transition from a coexisting state to a pure specialist state. We therefore see in both cases that flow shear will promote specialization. Parameter values for diffusion are $d_1 = d_2 = 5 \times 10^{-6}$ cm^2/s, $d_w = 15 \times 10^{-6}$ cm^2/s. For public good benefit, in the AND case, $a_{12} = 6.5 \times 10^{-3}$ s^{-1}, and in the OR case, $a_{12} = 7.5 \times 10^{-3}$ s^{-1}. The rest of the parameter values are given in Table 1

costs are low. In this case, cheaters 'chase after' producers, which grow into free space (Figure 5h and Video S6). High waste diffusion also helps cheaters, since they are able to chase producers without over-polluting themselves or their hosts (top-left regions in Figure 5a,b). When their invasion fitness is about equal to the producer growth rate, cheaters take over fully, driving the population to extinction (top-centre regions in Figure 5a,b). When the population aggregates into groups, cheater growth is limited to the group. Cooperation then prevails if groups reproduce faster than cheaters emerge. This happens when secretion costs are large. Remarkably, higher secretion costs can therefore stabilize specialist populations against cheater invasion (top-right regions in Figure 5a,b), since higher costs yield smaller groups which generate fewer mutations.

We see two regions of extinction: when public good benefit and waste diffusion are large, at medium costs (top-centre regions in

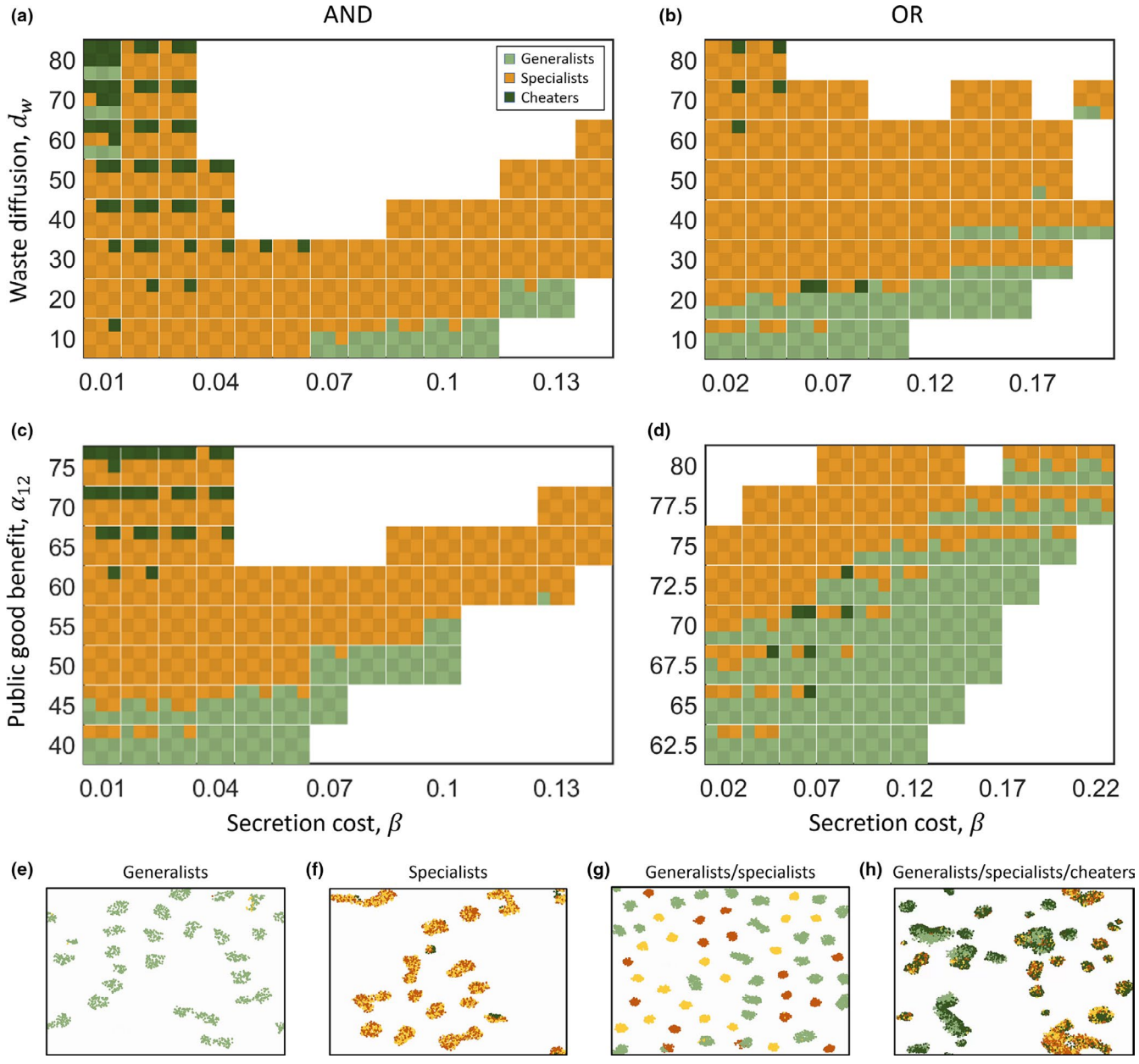

FIGURE 5 Effects of waste diffusion, public good benefit and cooperation cost on specialization. (a,b) Population composition for varying secretion cost β and waste diffusion d_w for AND (a) and OR fitness types (b). Each square is filled proportionally to the population composition of generalists, specialists and cheaters. When waste diffusion is larger than the public good diffusion, the population will form spatial structures. Under certain conditions, we see that generalists, specialists and cheaters coexist. At low costs, specialization and cheating are more abundant. At medium costs, cheaters spread faster than groups fragment, leading to extinction, shown as empty regions. At higher costs, specialists form smaller groups that fragment quicker than cheaters spread and are stable at steady state. Specialists do better overall when waste diffusion is large, since they can then form denser groups without over-polluting themselves. (c,d) Population compositions for varying secretion cost β and public good benefit a_{12} for AND (c) and OR fitness types (d). Higher public good benefit, a_{12}, also helps specialization, since secreting fewer public goods still gives a large benefit. Interestingly, higher benefit also leads to more extinct states, since cheaters can take over quicker. (e–h) Simulation snapshots for various possible stable populations. Under certain conditions, we can see (e), stable generalists, shown here for AND fitness (Video S1). Parameters here are $\beta = 0.12$, $d_1 = d_2 = 5 \times 10^{-6}$ cm^2/s, $d_w = 15 \times 10^{-6}$ cm^2/s, $a_{12} = 6.5 \times 10^{-3}$ s^{-1}. (f) Stable specialists in AND fitness (Video S3). Parameters here are $d_1 = d_2 = 5 \times 10^{-6}$ cm^2/s, $d_w = 15 \times 10^{-6}$ cm^2/s, $a_{12} = 6.5 \times 10^{-3}$ s^{-1} $\beta = 0.08$. (g) Generalists coexisting with specialists in OR fitness (Video S5). Parameter values $d_1 = d_2 = 25 \times 10^{-6}$ cm^2/s, $d_w = 40 \times 10^{-6}$ cm^2/s, $a_{12} = 6.5 \times 10^{-3}$ s^{-1}, $\beta = 0.14$, $\mu = 5 \times 10^{-8}$ s^{-1} (h) Coexistence of generalists, specialists and cheaters in AND fitness (Video S6). Parameter values $d_1 = d_2 = 20 \times 10^{-6}$ cm^2/s, $d_w = 60 \times 10^{-6}$ cm^2/s, $a_{12} = 7.5 \times 10^{-3}$ s^{-1}, $a_w = 105 \times 10^{-3}$ s^{-1}, $\beta = 0.02$, $\mu = 2 \times 10^{-7}$ s^{-1}. Population values were obtained by taking a time average over 1 run for each parameter value, over time steps $T = 1 \times 10^6$ s to $T = 2 \times 10^6$ s. Public good diffusion for the AND case (a,c) is $d_{12} = 20 \times 10^{-6}$ cm^2/s, for the OR case (b, d) $d_{12} = 25 \times 10^{-6}$ cm^2/s. Flow rate is set to 0, and other parameters are as given in Table 1

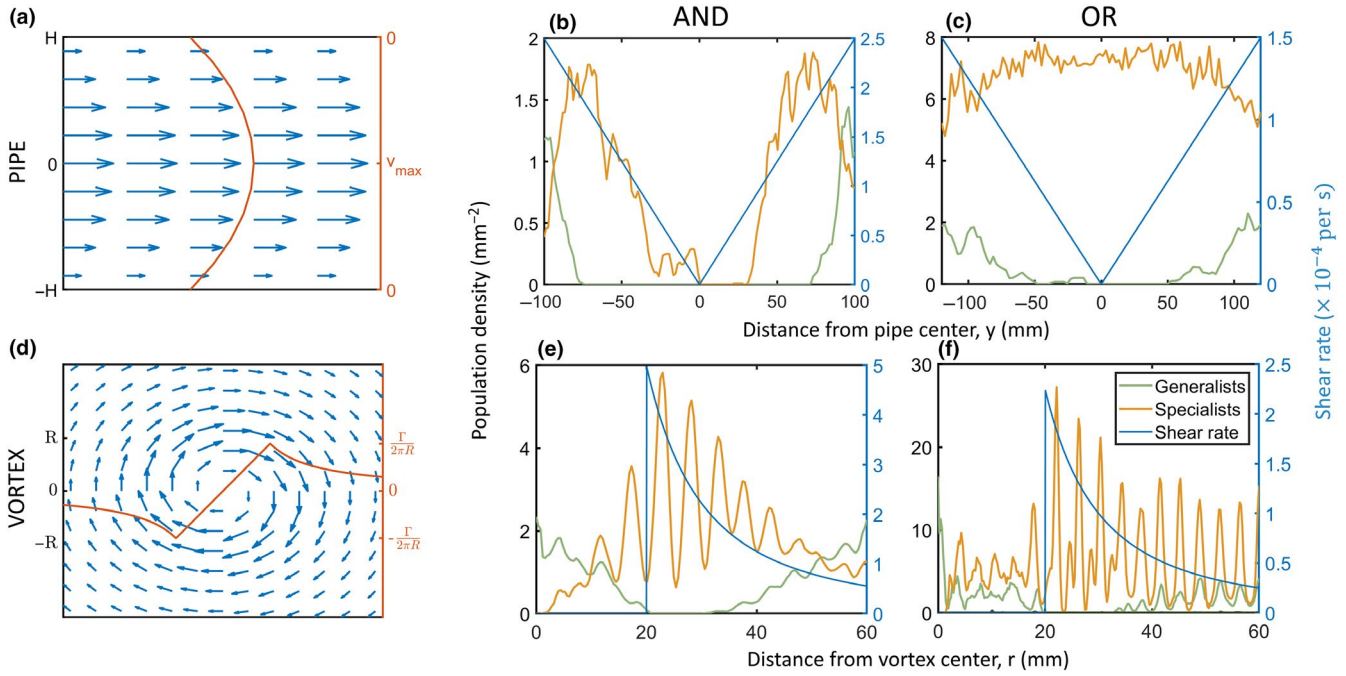

FIGURE 6 Coexistence of specialists and generalists in pipes and vortices. The local shear profile dictates which interaction structure is stable. When shear is spatially varying, we can get coexistence of generalists and specialists. (a) Schematic of Hagen–Poiseuille flow in a 2-dimensional pipe. (b) In the AND case in a pipe flow, we observe generalists residing at the boundaries followed by specialists towards the middle. In the centre where shear is lowest, cheaters quickly spread and consume groups, leading to a local tragedy of the commons. The population then goes extinct in the centre region (cf. Video S7). Flow parameters are H = 100 mm, v_{max} = 125 mm/s and mutation rate $\mu = 5 \times 10^{-7}$ s^{-1}. (c) For the OR case, in a pipe, generalists and specialists coexist at the boundary while specialists dominate the centre. Flow parameters for the OR case are H = 120 mm, v_{max} = 90 mm/s and mutation rate $\mu = 5 \times 10^{-8}$ s^{-1}. (d) Schematic of flow profile in Rankine vortex. (e) In a Rankine vortex flow, in the AND case we see generalists where shear is lowest, and specialists residing in an annulus where shear is at its maximum (cf. Video S8). Flow parameters for the vortex in the AND case are R = 20 mm, $\Gamma = 4000\pi$ mm^2/s and mutation rate $\mu = 3 \times 10^{-7}$ s^{-1}. (f) In the OR case, we see similar results, with coexistence of groups at low shear regions and an annular region composed of specialists. Flow parameters for the OR case are R = 20 mm and $\Gamma = 1{,}800\pi$ mm^2/s and mutation rate $\mu = 5 \times 10^{-8}$ s^{-1}. The total simulation domain for vortices was 60 mm × 60 mm. Secretion costs used are β = 0.12 for the AND fitness, and β = 0.17 for the OR fitness. Diffusion parameters used were $d_1 = d_2 = 5 \times 10^{-6}$ cm^2/s, $d_w = 15 \times 10^{-6}$ cm^2/s. Public good benefit in the AND case was $a_{12} = 6.5 \times 10^{-3}$ s^{-1} and for the OR case, $a_{12} = 7.5 \times 10^{-3}$ s^{-1}. The rest of the parameters are as given in Table 1. Population densities were obtained from averaging 5 runs at simulation time of $T = 2 \times 10^6$ s

Figure 5a-d), and when public good benefit and waste diffusion are low, at high costs (bottom-right regions in Figure 5a-d). The first case is due to cheaters taking over groups, leading to the tragedy of the commons. Interestingly, this occurs more with higher public good benefit. The population of producers becomes 'too fit' and more vulnerable to cheating mutations. For the second case, since costs are high and benefits are low, microbes need to form dense groups to utilize enough goods to be stable. However, due to the low waste diffusion, these groups over-pollute themselves and are no longer stable.

We see similar trends for both the AND (Figure 5a,c) and OR cases (Figure 5b,d). The main distinction between the two being, for the OR case, we predominately see pure specialist groups and only have mixed specialists in the AND case. We do not see many mixed specialists in the OR case since mutations take over generalists groups quicker and stabilize as pure groups, whereas in the AND case, pure groups would die out unless the complementary specialist also evolves in the same group. The AND structure is therefore essential to have true division of labour, where each type of specialist exists equally in the group.

3.5 | Localization of specialization and coexistence in axial and circular flows

We next study the evolution of specialization in axial (Hagen–Poiseuille, Figure 6a) and circular (Rankine vortex, Figure 6d) flows. Again, we set the cost parameter to a value where shear makes the biggest difference. As with the case with constant shear (Figure 4c,d), we set for AND fitness, β = 0.12 and for OR fitness, β = 0.17. For a Hagen–Poiseuille flow in a two-dimensional pipe, the flow rate and shear rate are given by,

$$v = v_{max}\left(1 - \frac{y^2}{H^2}\right)\hat{x}, \qquad \left|\frac{dv}{dy}\right| = \frac{2v_{max}y}{H^2}.$$

The flow pattern is in the $\hat{x}$ direction and maximal at the centre of the pipe, corresponding to y = 0. Because of no-slip boundary conditions, flow is zero at the boundaries of the pipe $y = \pm H$ (Figure 6a). The shear rate magnitude is given by taking the derivative of the flow rate with respect to y and varies linearly with distance y. The

shear rate is zero at the centre of the pipe and maximal at the boundaries of the pipe.

From our results with a constant shear (Figure 4c,d), we expect higher shear regions of the pipe to be occupied by specialists and lower shear regions to be occupied by generalists. However, we see the opposite to occur (Figure 6b,c). This is due to boundary and second-order effects. Generalist groups on the boundary fragment more often and are able to prevent takeover by mutations. Longer groups are formed in regions of intermediate shear and generate more mutations, leading to a predominately specialist population in this region (Figure 6b,c, Video S7). The fragmenting generalist groups act as a source for specialists groups in the intermediate regions of the pipe. Near the centre of the pipe where the shear rate is low, groups do not fragment as quickly and are taken over by cheaters. We therefore see a coexistence of group types across the pipes, with generalists at the boundary, followed by specialists in the intermediate regions (Figure 6b,c), and an extinct population due to groups being destroyed by cheaters at the centre (Figure 6b).

Next, we study evolution in a Rankine vortex. The flow and shear profiles for a Rankine vortex with radius R and circulation Γ are given by,

$$\mathbf{v}=\begin{cases}\frac{\Gamma r}{2\pi R^2}\hat{\theta}, & r\le R\\ \frac{\Gamma}{2\pi r}\hat{\theta}, & r>R\end{cases}\quad \sigma=\begin{cases}0, & r\le R\\ \frac{\Gamma}{2\pi r^2}\hat{\theta}, & r>R\end{cases}.$$

The flow pattern is now in the angular direction $\hat{\theta}$. The magnitude of flow increases linearly up to the vortex radius R and then drops as $1/r$, where $r=\sqrt{x^2+y^2}$ is the distance from the vortex centre (Figure 6d). The circulation parameter Γ corresponds to the line integral of the flow field along a closed path and has units of velocity times length. Here, we use it to tune the rate of flow and shear rate. The shear rate σ is in the radial direction. It is zero within the vortex $r < R$, maximal at the vortex radius $r = R$, and decreases as $1/r^2$ for $r > R$. There is no shear in the radial direction $\hat{r}$.

The distribution of specialists and generalists in the vortex agrees better with previous results from constant shear (Figure 6e,f). We see generalists persist in regions of low shear and specialists mainly reside in an annular region where shear is large (Figure 6e,f, Video S8). In either case, we see coexistence of communities with different interaction structures across the full domain. A varying shear profile can therefore allow for different group types to dominate different regions in the fluid and stably coexist in other regions.

4 | DISCUSSION

Fletcher and Doebeli, (2009) show that altruism is favoured when cooperators are more likely to interact with other cooperators and less likely to encounter cheaters. Such assortment can be attained when populations are viscous (Taylor, 1992) and spatially self-structured (Stump et al., 2018; Wakano et al., 2009). Kin selection is then the main driving evolutionary force of cooperation in spatially structured populations (Lion & Baalen, 2008). Our findings are consistent with these ideas.

More specifically, we have seen that invasion fitness alone does not govern the evolution of interactions within a community. Rather, physical dynamics governing the habitat and the microbes prove highly influential in whether specialized cooperation, generalized cooperation or cheating strategies will dominate, as well as whether multiple types of groups will coexist. We showed that the spatial structure and dynamical properties of communities, as modulated by diffusion constants, decay rates, fluid dynamical forces and domain geometry can outweigh the role of fitness economics. These physical factors give generalist cooperator groups a fighting chance against specialist cooperators, and generalist and specialist cooperators against cheaters. As such, we view division of labour as a mechanical phenomena as much as an economical one.

While analysing the competition between different interaction strategies within a community, we also investigated the competition between different kinds of communities. While a given niche with given physical parameters will be typically exclusively dominated by either generalist groups, specialist groups or cheaters, we also found that for a range of parameters, the physical and economical factors will counteract in a balanced way, leading to the coexistence of multiple interaction structures within one fluid niche.

A shearing flow can influence the evolution of cooperation in microbial populations (Nadell et al., 2017; Uppal & Vural, 2018). Here, we also saw that fluid flow can alter the spatial structure and dynamic properties of communities, and hence the evolution of their cooperative interactions. A shearing flow increases the group size of generalists and fragmentation rates of specialists and therefore alters the evolutionary stability of the community interaction structure. When the fluid shear profile varies over space, we observe that generalists and specialists not only find the most suitable position for themselves in the fluid and dominate there, they can also coexist in certain regions.

Many authors view undifferentiated multicellularity as a prerequisite for specialization (Bonner, 1998; Gavrilets, 2010; Michod, 2007; Pfeiffer & Bonhoeffer, 2003; Rossetti et al., 2010). In the case where generalists form a spatially homogeneous population and specialists form groups, we have seen that a transition to specialization can split the population into discrete subpopulations, that is functional multicellular groups. In this light, division of labour can be viewed as a first cause of multicellularity, rather than a consequence.

Though we paid close attention to physical realism, we also made important simplifying assumptions in our first-principles model. First, we assumed identical mutation rates between all pairs of phenotypes, whereas in reality, loss-of-function mutations are often more likely. Second, for most simulations we took the diffusion constants and decay rates of the two public goods to be identical. Studying cases where $d_1 \neq d_2$ or $\lambda_1 \neq \lambda_2$ could give additional interesting results that we have not explored here. Specifically, we think that the existence of a diffusion length blurs the distinction between public and private goods, and communities might end up with larger numbers of producers of the less diffusive (more private)

good and larger numbers of exploiters of the more diffusive (more public) good. We also neglect the finite sizes and complex shapes of microbes, and instead take them as point particles. Additionally, since microbes live in a low Reynolds number environment, we ignore the inertia of microbes, whereas in reality, microbes will themselves influence the fluid flow patterns. This effect will become especially important in highly dense populations and when microbes actively stick to one another or integrate via extracellular polymers. Finally, we neglect the taxis of microbes. In reality, microbes can exhibit complex swimming patterns and move towards or against chemical gradients.

Theoretical and experimental investigations of these additional factors will provide further insights into the interplay between mechanical factors and evolution of community interactions.

ACKNOWLEDGMENTS

This material is based upon work supported by the Defense Advanced Research Projects Agency under Contract No. HR0011-16-C-0062 and National Science Foundation grant CBET-1805157

ORCID

Gurdip Uppal https://orcid.org/0000-0003-3957-256X
Dervis Can Vural https://orcid.org/0000-0002-0495-8086

REFERENCES

Allen, R. C., McNally, L., Popat, R., & Brown, S. P. (2016). Quorum sensing protects bacterial co-operation from exploitation by cheats. *The ISME Journal*, *10*, 1706–1716.

Allen, R. J., & Waclaw, B. (2018). Bacterial growth: A statistical physicist's guide. *Reports on Progress in Physics*, *82*(1), 016601.

An, D., Danhorn, T., Fuqua, C., & Parsek, M. R. (2006). Quorum sensing and motility mediate interactions between *Pseudomonas aeruginosa* and *Agrobacterium tumefaciens* in biofilm cocultures. *Proceedings of the National Academy of Sciences of the United States of America*, *103*(10), 3828–3833.

Bachmann, H., Molenaar, D., Kleerebezem, M., & van Hylckama Vlieg, J. E. (2011). High local substrate availability stabilizes a cooperative trait. *The ISME Journal*, *5*(5), 929.

Beshers, S. N., & Fewell, J. H. (2001). Models of division of labor in social insects. *Annual Review of Entomology*, *46*(1), 413–440.

Biancalani, T., Fanelli, D., & Di Patti, F. (2010). Stochastic turing patterns in the brusselator model. *Physical Review E*, *81*(4), 046215.

Blat, Y., & Eisenbach, M. (1995). Tar-dependent and-independent pattern formation by *Salmonella typhimurium*. *Journal of Bacteriology*, *177*(7), 1683–1691.

Bonner, J. T. (1998). The origins of multicellularity. *Integrative Biology: Issues, News, and Reviews*, *1*(1), 27–36.

Budrene, E. O., & Berg, H. C. (1991). Complex patterns formed by motile cells of *Escherichia coli*. *Nature*, *349*(6310), 630.

Butler, T., & Goldenfeld, N. (2009). Robust ecological pattern formation induced by demographic noise. *Physical Review E*, *80*(3), 030902.

Carroll, S. B. (2001). Chance and necessity: The evolution of morphological complexity and diversity. *Nature*, *409*(6823), 1102.

Cooper, G. A., & West, S. A. (2018). Division of labour and the evolution of extreme specialization. *Nature Ecology & Evolution*, *2*(7), 1161.

Davies, D. (2003). Understanding biofilm resistance to antibacterial agents. *Nature Reviews Drug Discovery*, *2*(2), 114.

Dobay, A., Bagheri, H., Messina, A., Kümmerli, R., & Rankin, D. (2014). Interaction effects of cell diffusion, cell density and public goods properties on the evolution of cooperation in digital microbes. *Journal of Evolutionary Biology*, *27*(9), 1869–1877.

Dragoš, A., Kiesewalter, H., Martin, M., Hsu, C.-Y., Hartmann, R., Wechsler, T., … Kovács, Á. T. (2018). Division of labor during biofilm matrix production. *Current Biology*, *28*(12), 1903–1913.

Drake, J. W., Charlesworth, B., Charlesworth, D., & Crow, J. F. (1998). Rates of spontaneous mutation. *Genetics*, *148*(4), 1667–1686.

Durrett, R., & Levin, S. (1994). The importance of being discrete (and spatial). *Theoretical Population Biology*, *46*(3), 363–394.

Fletcher, J. A., & Doebeli, M. (2009). A simple and general explanation for the evolution of altruism. *Proceedings of the Royal Society of London B: Biological Sciences*, *276*(1654), 13–19.

Fu, X., Kato, S., Long, J., Mattingly, H. H., He, C., Vural, D. C., … Emonet, T. (2018). Spatial self-organization resolves conflicts between individuality and collective migration. *Nature Communications*, *9*(1), 2177.

Futuyma, D. J., & Moreno, G. (1988). The evolution of ecological specialization. *Annual Review of Ecology and Systematics*, *19*(1), 207–233.

Gavrilets, S. (2010). Rapid transition towards the division of labor via evolution of developmental plasticity. *PLoS Computational Biology*, *6*(6), e1000805.

Gibson, B., Wilson, D. J., Feil, E., & Eyre-Walker, A. (2018). The distribution of bacterial doubling times in the wild. *Proceedings of the Royal Society B: Biological Sciences*, *285*(1880), 20180789.

Goldsby, H. J., Dornhaus, A., Kerr, B., & Ofria, C. (2012). Task-switching costs promote the evolution of division of labor and shifts in individuality. *Proceedings of the National Academy of Sciences of the United States of America*, *109*(34), 13686–13691.

Greig, D., & Travisano, M. (2004). The prisoner's dilemma and polymorphism in yeast suc genes. *Proceedings of the Royal Society of London B: Biological Sciences*, *271*(Suppl 3), S25–S26.

Griffin, A. S., West, S. A., & Buckling, A. (2004). Cooperation and competition in pathogenic bacteria. *Nature*, *430*(7003), 1024.

Guerinot, M. L. (1994). Microbial iron transport. *Annual Reviews in Microbiology*, *48*(1), 743–772.

Harrison, F., & Buckling, A. (2009). Cooperative production of siderophores by *Pseudomonas aeruginosa*. *Frontiers in Bioscience*, *14*(14), 4113–4126.

Hedges, S. B., Blair, J. E., Venturi, M. L., & Shoe, J. L. (2004). A molecular timescale of eukaryote evolution and the rise of complex multicellular life. *BMC Evolutionary Biology*, *4*(1), 2.

Inglis, R. F., Gardner, A., Cornelis, P., & Buckling, A. (2009). Spite and virulence in the bacterium *Pseudomonas aeruginosa*. *Proceedings of the National Academy of Sciences of the United States of America*, *106*(14), 5703–5707.

Ispolatov, I., Ackermann, M., & Doebeli, M. (2012). Division of labour and the evolution of multicellularity. *Proceedings of the Royal Society of London B: Biological Sciences*, *279*(1734), 1768–1776.

Karig, D., Martini, K. M., Lu, T., DeLateur, N. A., Goldenfeld, N., & Weiss, R. (2018). Stochastic turing patterns in a synthetic bacterial population. *Proceedings of the National Academy of Sciences of the United States of America*, *115*(26), 6572–6577.

Kearns, D. B. (2010). A field guide to bacterial swarming motility. *Nature Reviews Microbiology*, *8*(9), 634.

Kim, Y.-C. (1996). Diffusivity of bacteria. *Korean Journal of Chemical Engineering*, *13*(3), 282–287.

Kirk, D. L. (2001). Germ–soma differentiation in volvox. *Developmental Biology*, *238*(2), 213–223.

Kirk, D. L., & Kirk, M. M. (1983). Protein synthetic patterns during the asexual life cycle of *Volvox carteri*. *Developmental Biology*, *96*(2), 493–506.

Kohler, T., Buckling, A., & van Delden C. (2009). Cooperation and virulence of clinical *Pseudomonas aeruginosa* populations. *Proceedings of the National Academy of Sciences of the United States of America*, *106*(14), 6339–6344.

Koufopanou, V. (1994). The evolution of soma in the volvocales. *The American Naturalist*, *143*(5), 907–931.

Kümmerli, R. B. S. (2010). Molecular and regulatory properties of a public good shape the evolution of cooperation. *Proceedings of the National Academy of Sciences of the United States of America*, *107*(107), 18921–18926.

Kutschera, U., & Niklas, K. J. (2005). Endosymbiosis, cell evolution, and speciation. *Theory in Biosciences*, *124*(1), 1–24.

Lewis, K. (2007). Persister cells, dormancy and infectious disease. *Nature Reviews Microbiology*, *5*(1), 48.

Lion, S., & Baalen, M. V. (2008). Self-structuring in spatial evolutionary ecology. *Ecology Letters*, *11*(3), 277–295.

Ma, Y., Zhu, C., Ma, P., & Yu, K. (2005). Studies on the diffusion coefficients of amino acids in aqueous solutions. *Journal of Chemical & Engineering Data*, *50*(4), 1192–1196.

Mah, T.-F.-C., & O'toole, G. A. (2001). Mechanisms of biofilm resistance to antimicrobial agents. *Trends in Microbiology*, *9*(1), 34–39.

May, R. M., & Seger, J. (1986). Ideas in ecology. *American Scientist*, *74*(3), 256–267.

Mazzola, M., Cook, R., Thomashow, L., Weller, D., & Pierson, L. (1992). Contribution of phenazine antibiotic biosynthesis to the ecological competence of fluorescent pseudomonads in soil habitats. *Applied and Environmental Microbiology*, *58*(8), 2616–2624.

McNally, L., Bernardy, E., Thomas, J., Kalziqi, A., Pentz, J., Brown, S. P., … Ratcliff, W. C. (2017). Killing by type VI secretion drives genetic phase separation and correlates with increased cooperation. *Nature Communications*, *8*, 14371.

Mendelson, N. H., & Lega, J. (1998). A complex pattern of traveling stripes is produced by swimming cells of *Bacillus subtilis*. *Journal of Bacteriology*, *180*(13), 3285–3294.

Menon, R., & Korolev, K. S. (2015). Public good diffusion limits microbial mutualism. *Physical Review Letters*, *114*(16), 168102.

Michod, R. E. (2007). Evolution of individuality during the transition from unicellular to multicellular life. *Proceedings of the National Academy of Sciences of the United States of America*, *104*(suppl 1), 8613–8618.

Michod, R. E., Viossat, Y., Solari, C. A., Hurand, M., & Nedelcu, A. M. (2006). Life-history evolution and the origin of multicellularity. *Journal of Theoretical Biology*, *239*(2), 257–272.

Monod, J. (1949). The growth of bacterial cultures. *Annual Reviews in Microbiology*, *3*(1), 371–394.

Moons, P., Van Houdt, R., Aertsen, A., Vanoirbeek, K., Engelborghs, Y., & Michiels, C. W. (2006). Role of quorum sensing and antimicrobial component production by *Serratia plymuthica* in formation of biofilms, including mixed biofilms with *Escherichia coli*. *Applied and Environmental Microbiology*, *72*(11), 7294–7300.

Moons, P., Van Houdt, R., Aertsen, A., Vanoirbeek, K., & Michiels, C. (2005). Quorum sensing dependent production of antimicrobial component influences establishment of e. coli in dual species biofilms with *Serratia plymuthica*. *Communications in Agricultural and Applied Biological Sciences*, *70*(2), 195.

Morris, J. J., Lenski, R. E., & Zinser, E. R. (2012). The black queen hypothesis: Evolution of dependencies through adaptive gene loss. *MBio*, *3*(2), e00036–e112.

Nadell, C. D., Ricaurte, D., Yan, J., Drescher, K., & Bassler, B. L. (2017). Flow environment and matrix structure interact to determine spatial competition in *Pseudomonas aeruginosa* biofilms. *Elife*, *6*, e21855.

Neilands, J. B. (1984). Siderophores of bacteria and fungi. *Microbiological Sciences*, *1*(1), 9–14.

Oliveira, N. M., Niehus, R., & Foster, K. R. (2014). Evolutionary limits to cooperation in microbial communities. *Proceedings of the National Academy of Sciences of the United States of America*, *111*(50), 17941–17946.

Pfeiffer, T., & Bonhoeffer, S. (2003). An evolutionary scenario for the transition to undifferentiated multicellularity. *Proceedings of the National Academy of Sciences of the United States of America*, *100*(3), 1095–1098.

Pirhonen, M., Flego, D., Heikinheimo, R., & Palva, E. T. (1993). A small diffusible signal molecule is responsible for the global control of virulence and exoenzyme production in the plant pathogen *Erwinia carotovora*. *The EMBO Journal*, *12*(6), 2467–2476.

Ratledge, C., & Dover, L. G. (2000). Iron metabolism in pathogenic bacteria. *Annual Reviews in Microbiology*, *54*(1), 881–941.

Rossetti, V., Schirrmeister, B. E., Bernasconi, M. V., & Bagheri, H. C. (2010). The evolutionary path to terminal differentiation and division of labor in cyanobacteria. *Journal of Theoretical Biology*, *262*(1), 23–34.

Rueffler, C., Hermisson, J., & Wagner, G. P. (2012). Evolution of functional specialization and division of labor. *Proceedings of the National Academy of Sciences of the United States of America*, *109*(6), E326–E335.

Rusconi, R., & Stocker, R. (2015). Microbes in flow. *Current Opinion in Microbiology*, *25*, 1–8.

Sachs, J., & Hollowell, A. (2012). The origins of cooperative bacterial communities. *MBio*, *3*(3), e00099–e112.

Sandoz, K. M., Mitzimberg, S. M., & Schuster, M. (2007). Social cheating in *Pseudomonas aeruginosa* quorum sensing. *Proceedings of the National Academy of Sciences of the United States of America*, *104*(40), 15876–15881.

Schiessl, K. T., Ross-Gillespie, A., Cornforth, D. M., Weigert, M., Bigosch, C., Brown, S. P., … Kümmerli, R. (2019). Individual-versus group-optimality in the production of secreted bacterial compounds. *Evolution*, *73*(4), 675–688.

Siegel, R. (1960). Hereditary endosymbiosis in *Paramecium bursaria*. *Experimental Cell Research*, *19*(2), 239–252.

Smith, C. R., Toth, A. L., Suarez, A. V., & Robinson, G. E. (2008). Genetic and genomic analyses of the division of labour in insect societies. *Nature Reviews Genetics*, *9*(10), 735.

Solari, C. A., Kessler, J. O., & Goldstein, R. E. (2013). A general allometric and life-history model for cellular differentiation in the transition to multicellularity. *The American Naturalist*, *181*(3), 369–380.

Solari, C. A., Kessler, J. O., & Michod, R. E. (2006). A hydrodynamics approach to the evolution of multicellularity: Flagellar motility and germ-soma differentiation in volvocalean green algae. *The American Naturalist*, *167*(4), 537–554.

Sriswasdi, S., Yang, C.-C., & Iwasaki, W. (2017). Generalist species drive microbial dispersion and evolution. *Nature Communications*, *8*(1), 1162.

Stump, S. M., Johnson, E. C., & Klausmeier, C. A. (2018). Local interactions and self-organized spatial patterns stabilize microbial cross-feeding against cheaters. *Journal of the Royal Society Interface*, *15*(140), 20170822.

Tannenbaum, E. (2007). When does division of labor lead to increased system output? *Journal of Theoretical Biology*, *247*(3), 413–425. https://doi.org/10.1016/j.jtbi.2007.03.020

Taylor, P. D. (1992). Altruism in viscous populations—an inclusive fitness model. *Evolutionary Ecology*, *6*(4), 352–356.

Terborgh, J., & Robinson, S. (1986). Guilds and their utility in ecology. In J. Kikkawa & D. J. A. Anderson (Eds.), *Community ecology: Pattern and process* (pp. 65–90). Oxford, UK: Blackwell Scientific Publications.

Tsimring, L., Levine, H., Aranson, I., Ben-Jacob, E., Cohen, I., Shochet, O., & Reynolds, W. N. (1995). Aggregation patterns in stressed bacteria. *Physical Review Letters*, *75*(9), 1859.

Uppal, G., & Vural, D. C. (2018). Shearing in flow environment promotes evolution of social behavior in microbial populations. *eLife*, *7*, e34862.

Vural, D. C., Isakov, A., & Mahadevan, L. (2015). The organization and control of an evolving interdependent population. *Journal of the Royal Society Interface*, *12*(108):20150044.

Wakano, J. Y., Nowak, M. A., & Hauert, C. (2009). Spatial dynamics of ecological public goods. *Proceedings of the National Academy of Sciences of the United States of America*, *106*(19), 7910–7914.

West, S. A., Diggle, S. P., Buckling, A., Gardner, A., & Griffin, A. S. (2007). The social lives of microbes. *Annual Review of Ecology, Evolution, and Systematics*, *38*, 53–77.

West, S. A., Fisher, R. M., Gardner, A., & Kiers, E. T. (2015). Major evolutionary transitions in individuality. *Proceedings of the National Academy of Sciences of the United States of America*, *112*(33), 10112–10119.

Willensdorfer, M. (2008). Organism size promotes the evolution of specialized cells in multicellular digital organisms. *Journal of Evolutionary Biology*, *21*(1), 104–110.

Willensdorfer, M. (2009). On the evolution of differentiated multicellularity. *Evolution: International Journal of Organic Evolution*, *63*(2), 306–323.

Wilson, W., Morris, W., & Bronstein, J. (2003). Coexistence of mutualists and exploiters on spatial landscapes. *Ecological Monographs*, *73*(3), 397–413.

Xavier, J. B., Kim, W., & Foster, K. R. (2011). A molecular mechanism that stabilizes cooperative secretions in *Pseudomonas aeruginosa*. *Molecular Microbiology*, *79*(1), 166–179.

Xue, Z., Sendamangalam, V. R., Gruden, C. L., & Seo, Y. (2012). Multiple roles of extracellular polymeric substances on resistance of biofilm and detached clusters. *Environmental Science & Technology*, *46*(24), 13212–13219.

Zelezniak, A., Andrejev, S., Ponomarova, O., Mende, D. R., Bork, P., & Patil, K. R. (2015). Metabolic dependencies drive species co-occurrence in diverse microbial communities. *Proceedings of the National Academy of Sciences of the United States of America*, *112*(20), 6449–6454.

Zhu, J., Miller, M. B., Vance, R. E., Dziejman, M., Bassler, B. L., & Mekalanos, J. J. (2002). Quorum-sensing regulators control virulence gene expression in vibrio cholerae. *Proceedings of the National Academy of Sciences of the United States of America*, *99*(5), 3129–3134.

SUPPORTING INFORMATION

Additional supporting information may be found online in the Supporting Information section.

How to cite this article: Uppal G, Vural DC. Evolution of specialized microbial cooperation in dynamic fluids. *J Evol Biol*. 2020;33:256–269. https://doi.org/10.1111/jeb.13593